Development 134, 3283-3295 (2007) doi:10.1242/dev.005132

Wnt signaling mediates regional specification in the vertebrate face

Samantha A. Brugmann[1], L. Henry Goodnough[1], Alex Gregorieff[2], Philipp Leucht[1], Derk ten Berge[3], Christophe Fuerer[3], Hans Clevers[2], Roel Nusse[3] and Jill A. Helms[1,*]

At early stages of development, the faces of vertebrate embryos look remarkably similar, yet within a very short timeframe they adopt species-specific facial characteristics. What are the mechanisms underlying this regional specification of the vertebrate face? Using transgenic Wnt reporter embryos we found a highly conserved pattern of Wnt responsiveness in the developing mouse face that later corresponded to derivatives of the frontonasal and maxillary prominences. We explored the consequences of disrupting Wnt signaling, first using a genetic approach. Mice carrying compound null mutations in the nuclear mediators Lef1 and Tcf4 exhibited radically altered facial features that culminated in a hyperteloric appearance and a foreshortened midface. We also used a biochemical approach to perturb Wnt signaling and found that in utero delivery of a Wnt antagonist, Dkk1, produced similar midfacial malformations. We tested the hypothesis that Wnt signaling is an evolutionarily conserved mechanism controlling facial morphogenesis by determining the pattern of Wnt responsiveness in avian faces, and then by evaluating the consequences of Wnt inhibition in the chick face. Collectively, these data elucidate a new role for Wnt signaling in regional specification of the vertebrate face, and suggest possible mechanisms whereby species-specific facial features are generated.

KEY WORDS: Wnt, Craniofacial, Patterning, Axes formation, Maxilla, Frontonasal prominence, Species-specific facial features

INTRODUCTION

An embryo acquires species-specific facial characteristics fairly early during development, after which its external appearance changes little except for a considerable increase in size. Remarkable as this growth process is, one of the greatest unsolved mysteries of development is the control of morphogenetic movements that establish order and pattern. This process lies at the heart of embryology, and is the mechanism by which a simple sheet of cells is transformed into an embryo with a readily discernable anterior end.

It is the anterior portion of the embryo that gives rise to the face. How the face achieves its own distinctive pattern is obviously a complex problem and has puzzled a great number of scientists. In general, the problem can be stated as one of regional specification: what are the distinguishing characteristics that allow us to readily discriminate an embryonic mouse face from a chick face? And when does this regional specification occur?

One could consider that as soon as the anterior end of an embryo is patterned then craniofacial morphogenesis is under species-specific control (Schneider and Helms, 2003) (reviewed by Helms and Schneider, 2003; Le Douarin et al., 2004). On the other hand, numerous experiments point to the plasticity inherent in the head region (Hu et al., 2003; Hunt et al., 1998; Trainor et al., 2002; Trainor et al., 1994). A multifarious hierarchy of signaling and responses between epithelium and mesenchyme gradually build up a complex pattern that culminates in species-specific facial features (e.g. Noden, 1988), but how does it all begin? Preeminent in understanding what molecular signals control regional specification within the craniofacial complex is first appreciating just how similar embryonic faces start out and how, within a relatively short time span, they become so different. This query is not without precedence: scientists have been investigating the mechanisms of craniofacial regional specification for centuries. Initially, such inquiries were dependent upon embryological manipulations, but more recently molecular biology and developmental genetics have also been used to shed light on the process of craniofacial morphogenesis.

The concept of a 'zootype' was proposed to describe a stage of embryonic development in which a particular spatial pattern of gene expression was responsible for establishing regional specification (Slack et al., 1993). In its original form, the zootype was defined by a spatially restricted class of homeobox genes, but the concept can easily be applied to other genes whose regional expression is conserved among and between species. The function of many of these genes is to provide positional information and this method of regional specification is highly conserved among different animal taxa (reviewed by Deschamps and van Nes, 2005) and is therefore probably very ancient.

Wnt proteins represent one of the most highly conserved molecular pathways known to man. From hydra to humans, Wnts play indisputably important roles in patterning and morphogenesis (Cadigan and Nusse, 1997) and there is an abundance of molecular tools available with which to investigate Wnt signaling. Here, we exploited some of these tools to gain insights into the role of Wnts in controlling regional specification in the craniofacial complex. We used transgenic Wnt reporter mice to map the patterns of Wnt responsiveness in the developing face and then undertook both a genetic approach and a biochemical strategy to explore the craniofacial consequences of Wnt perturbation. Finally, we experimentally tested our proposed model of Wnt signaling in a different animal model, the chick, and in doing so found clues as to the conserved nature of Wnt function in regional specification of the face.

[1]Department of Plastic and Reconstructive Surgery, Stanford University, Stanford, CA 94305, USA. [2]Hubrecht Laboratory, Netherlands Institute for Developmental Biology, Uppsalalaan 8, 3584 CT Utrecht, The Netherlands. [3]Howard Hughes Medical Institution, Stanford University, Stanford, CA 94305, USA.

*Author for correspondence (e-mail: jhelms@stanford.edu)

Accepted 27 June 2007

MATERIALS AND METHODS

Generating *Lef1*$^{-/-}$; *Tcf4*$^{-/-}$ embryos

The *Lef1*-null allele (van Genderen et al., 1994) and the disruption of *Tcf4* (Korinek et al., 1998b) were generated as previously described. Genotyping was performed by PCR of genomic DNA isolated from tail biopsies. The primers for the wild-type *Tcf4* allele were 5′-CAGCTCAAAGCATC-AGGACTC-3′ and 5′-GCGCCCGAGAATCTGGTTGATGG-3′; the null allele was amplified with primers specific for hygromycin: 5′-ACCTGC-CTGAAACCGAACTGC-3′ and GCGTCTGCTGCTCCATACAAG-3′. For *Lef1*, three primers detected the 100 bp wild-type and 300 bp mutant amplicons: 5′-CCGTTTCAGTGGCACGCCCTCTCC-3′, 5′-ATGGC-GATGCCTGCTTGCCGAATA-3′ and 5′-TGTCTCTCTTTCCGTGCTA-GTTC-3′. *Lef1*$^{-/-}$; *Tcf4*$^{-/-}$ embryos were bred by mating Lef1$^{+/-}$; *Tcf4*$^{+/-}$ animals.

TOPgal and BATgal embryos

TOPgal and BATgal mice were generated as previously reported (DasGupta and Fuchs, 1999; Maretto et al., 2003).

Detection of *lacZ* expression

β-galactosidase (β-gal) hydrolyzes the non-inducing chromogenic substrate 5-bromo-4-chloro-3-indolyl-beta-D-galactopyranoside (X-Gal; Invitrogen, Carlsbad, CA) to form a blue precipitate. To visualize the enzyme's expression, freshly collected tissues were rinsed in PBS, fixed with 0.2% glutaraldehyde for 15 minutes, and stained with X-Gal overnight in whole-mount at 37°C (Maretto et al., 2003). For tissue sections, freshly collected embryos were fixed in 0.4% paraformaldehyde (PFA) for 2 hours and infused with 30% sucrose for 24 hours. Samples were then embedded in OCT medium, frozen with dry ice in isopentane, and stored at –80°C before cryosectioning. X-Gal staining for cryosections followed the whole-mount protocol.

Adenovirus production and in utero injection

Adenovirus containing the Wnt inhibitor Dkk1 was generated as previously reported (Kuhnert et al., 2004). 293T cells were transfected with Ad-Dkk1 construct following standardized purification, concentration and titering steps. In brief, pregnant TOPgal females were anesthetized and a laparotomy was performed to expose the uterine horns. One horn was deflected onto the ventral abdominal surface and alternate embryos of the uterine horn were injected to avoid excessive loss of amniotic fluid. Approximately 4×10^9 virions (2 μL) were injected into individual uteri according to previously reported protocols (Itah et al., 2004). Embryos were harvested 4 days post-injection.

Lentivirus production and in ovo injection

A DNA fragment containing seven Tcf/Lef-binding sites, the minimal promoter and the 5′UTR of the pSuperTOPflash reporter plasmid (Veeman et al., 2003) was amplified by PCR and inserted upstream of the eGFP gene in the self-inactivating lentivirus TOP-eGFP (Reya et al., 2003). Vectors were produced by transient transfection in 293T cells. Briefly, ten 10-cm dishes were seeded with 5×10^6 cells each, the day before transfection. For each dish, 10 μg of the virus construct were mixed with 3.5 μg of the VSV-G envelope plasmid and 6.5 μg of the packaging plasmid (pMD2.VSVG and pCMVΔR8.74, respectively) (Dull et al., 1998). The solution was adjusted to 250 μL with water and mixed with 250 μL 0.5 M $CaCl_2$. The precipitate was formed by adding drop-wise while vortexing 500 μL of 2×HEPES-buffered saline (280 mM NaCl, 10 mM KCl, 1.5 mM Na_2HPO_4, 12 mM dextrose, 50 mM HEPES, pH7.2) and was added directly to the cells. The medium was replaced after 16 hours and conditioned twice for 24 hours. The conditioned media were pooled, filtered through a 0.45 μm PES filter, and centrifuged at 50,000***g*** for 2 hours 20 minutes. The viral pellet was resuspended in 400 μL 0.1% BSA in PBS. In ovo injections of Ad-Dkk1 and pLenti 7xTcf-eGFP were performed at stages 10 and 13, respectively. Approximately 2 μL of virus (4×10^9 virions for Ad-Dkk1 and 1×10^4 virions for pLenti 7xTcf-eGFP) was applied to the surface ectoderm anterior region of the embryo and injected into developing facial prominences.

In situ hybridization

Embryos were fixed in 4% PFA overnight at 4°C, dehydrated serially to 100% methanol, and for whole-mounts, rehydrated in PBS at room temperature. For tissue sections, dehydrated embryos were embedded in paraffin and sectioned at 8 μm. Templates for the relevant mRNAs for in situ hybridization were amplified from embryonic mouse cDNA by PCR using sequence-specific primers that included the promoter sites for T3 or T7 RNA polymerase. Antisense riboprobe for each gene was transcribed with either T3 or T7 RNA polymerase in the presence of Dig-11-UTP (Roche, Indianapolis, IN). Whole-mount and section in situ hybridizations (Albrecht et al., 1997) were performed as described previously. Briefly, tissue sections or whole-mount embryos were incubated at 70°C for 12 hours in hybridization buffer (Ambion Corporation, Austin, TX) containing riboprobe at ~0.2-0.3 μg/mL probe per kb of probe complexity. Non-specifically bound probe was hydrolyzed with RNase A, and final washes were carried out at high stringency (0.1×SSC, 65°C). For color detection, embryos or slides were blocked with 10% sheep serum, 1% Boehringer-Mannheim Blocking Reagent (Roche) and levamisole, and developed using nitro blue tetrazolium chloride (NBT; Roche) and 5-bromo-4-chloro-3-indolyl phosphate (BCIP; Roche). After developing, the slides were cover-slipped with aqueous mounting medium.

RESULTS

Mapping Wnt responsiveness during craniofacial morphogenesis

Our first objective was to determine the spatiotemporal patterns of Wnt signaling in the face. There are a number of transgenic strains of mice in which reporter activity is a reflection of endogenous Wnt signaling (DasGupta and Fuchs, 1999; Maretto et al., 2003; Moriyama et al., 2007; Reya et al., 2003). In BATgal and TOPgal embryos, the β-gal reporter gene is under the control of Lef/Tcf-binding sites. The primary differences between the two strains are the type of promoter used, and the number of Lef/Tcf-binding sites (DasGupta and Fuchs, 1999; Maretto et al., 2003). When we examined BATgal and TOPgal embryos for the pattern of β-gal activity in the head, we found a general conservation in the location of staining, but there were notable differences as well (Fig. 1). For example, at E9.5, both transgenic embryos showed strong reporter activity in the midbrain and anterior neural folds, and lesser amounts of staining in the anterior surface ectoderm (Fig. 1A,D, dotted white lines). In addition, there were differences in the intensity of staining in the head (Fig. 1, compare B with C). There were, however, areas where the staining pattern was conserved: the first pharyngeal arch was β-gal-positive and, in general, the most anterior region of the face had little X-Gal staining (Fig. 1B,C). At later stages of development, we once again noted similarities and differences in the pattern of reporter activity in TOPgal and BATgal embryos. For example, at E14.5 there was a discernable variation in the forebrain pattern of X-Gal staining, although both embryos showed reporter activity in the dorsal-most region (Fig. 1E,H), but along with this variation was an equally notable conservation in the pattern of reporter activity within the developing craniofacial complex. Specifically, both transgenes were expressed in the maxillary prominences, a stripe along the lateral nasal prominences, and within a small patch in the median nasal prominence (Fig. 1F,G). Likewise, both embryos showed reporter activity in discrete domains such as the junction between the maxillary and mandibular prominences (Fig. 1F,G, arrowheads), in the otic placode (Fig. 1F,G, asterisk), and in the aboral surface of the mandible (Fig. 1F,G, arrows). This striking similarity in Wnt reporter activity was observed again, at E14.5, in the face and in specialized epithelial structures in the face such as the whisker primordia (Fig. 1I-L), taste buds and tooth buds. As before, subtle differences in X-Gal staining could be detected between TOPgal and BATgal embryos, but despite these differences there was one common feature: the facial midline was devoid of Wnt reporter activity, whereas the lateral regions

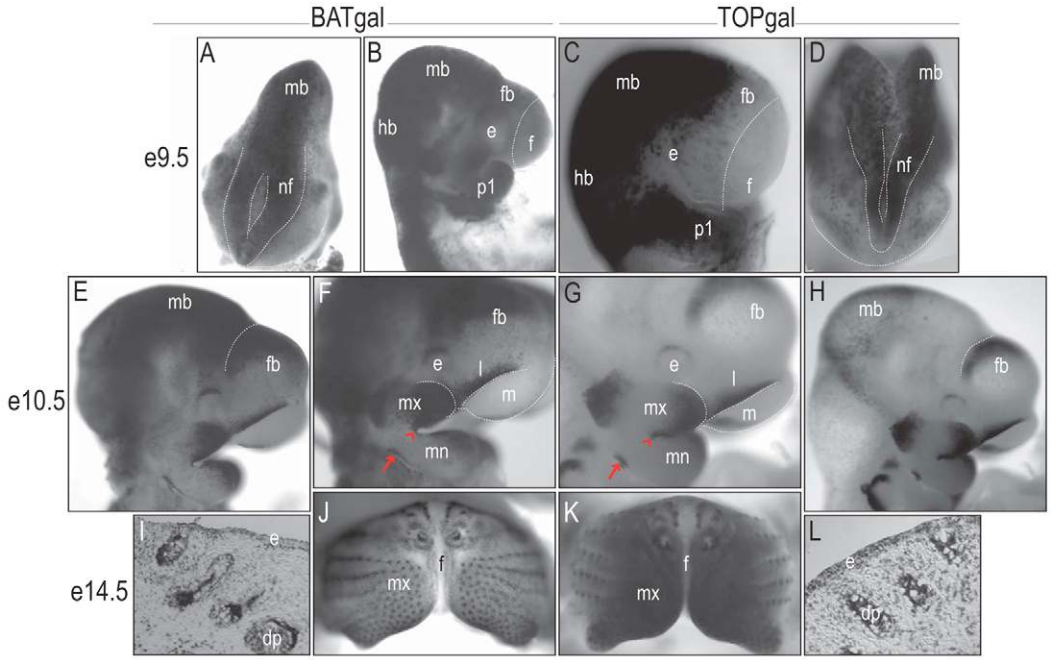

Fig. 1. Comparisons between X-Gal staining patterns in Wnt reporter mice. (**A-D**) X-Gal staining for Wnt reporter activity at E9.5. (A) Staining is evident in the midbrain (mb) and anterior neural folds (nf) of BATgal embryos. (B) A lateral view shows reporter activity in the first pharyngeal arch (p1). (C) In TOPgal embryos, Wnt reporter activity is evident in the first pharyngeal arch (p1) as well as the midbrain (mb) and hindbrain (hb). No Wnt reporter activity is detectable in the anterior region of the face (f). (D) Wnt reporter activity in the midbrain (mb) and anterior neural folds (nf) of TOPgal embryos generally mirrors that seen in BATgal embryos. Note that the BATgal and TOPgal embryos are at slightly different stages of development, as gauged by the extent of neural tube fusion (dotted white lines, A and D). (**E-H**) X-Gal staining at E10.5. (E) Wnt reporter activity is evident in the midbrain (mb) and forebrain (fb) of BATgal embryos. (F) Reporter activity is also evident in the distal regions of the maxillary (mx) and mandibular (mn) prominences, the aboral surface of the mandible (red arrow), the proximal first arch (red arrowhead), the lateral nasal (l) prominences, and around the developing eye (e). (G) A nearly identical pattern of reporter activity is seen in the TOPgal face. (H) One subtle difference in reporter activity at this stage is in the forebrain region, where X-Gal staining appears more restricted than that observed in BATgal embryos (compare E with H). (**I-L**) X-Gal staining at E14.5. (I) Wnt reporter activity is evident in surface ectoderm overlying the dermal papilla, signaling the site of whisker development. (J) At the same stage, Wnt reporter activity is abundant in the maxillary (mx) prominences but absent in the frontonasal (f) prominence. (K,L) The pattern of Wnt reporter activity in the TOPgal face and whisker primordia mirrors that seen in BATgal embryos at the same stage.

exhibited exuberant Wnt reporter activity (Fig. 1J,K). It was this aspect of the X-Gal staining that became the focus of our next experiments, as we sought to understand how the pattern becomes established in the face.

We began by examining β-gal activity in TOPgal embryos from around neurulation (~E8.5). At this time, the anterior neural plate showed evidence of strong X-Gal staining in the lateral regions (Fig. 2A,B) and tissue sections revealed that X-Gal staining was limited to the ectoderm of the neural folds (Fig. 2C). This ectoderm later becomes subdivided into both neuroectoderm and surface ectoderm (Brugmann et al., 2006). At E9.5, X-Gal staining was detectable in the surface ectoderm and the delaminating cranial neural crest cells (Fig. 2D-F). By E10.5, these cranial neural crest cells have completed their migration into the facial prominences. X-Gal staining was evident in all of the prominences with the singular exception of the frontonasal (Fig. 2G,H). Tissue sections showed β-gal-positive cells in both surface ectoderm and mesenchyme of the maxillae, but, in accordance with the whole-mount staining, reporter activity was undetectable in the frontonasal (Fig. 2I). At E11.5, the median nasal prominence fuses with the lateral nasal and maxillary prominences (Fig. 2J,K). We carefully mapped Wnt reporter activity at this point and noted the presence of β-gal-positive cells in maxillary ectoderm and mesenchyme, and the absence of β-gal-positive cells in the median nasal prominence (Fig. 2L). Even after the prominences had fused, X-Gal staining remained in the mesenchyme of the maxillary prominence, but we found no staining in the frontonasal (Fig. 2L). By E12.0, the facial prominences have coalesced (Fig. 2M) and, as before, reporter activity was conspicuously lacking in the frontonasal prominence (Fig. 2N). The same pattern was readily discernable at E12.5 (Fig. 2O,P). At this developmental stage there is no morphological structure that corresponds to this boundary between reporter-positive and reporter-negative regions in the face.

With advancing embryonic age, we found that the molecular demarcation between β-gal-positive and β-gal-negative cells precisely correlated with derivatives of the frontonasal and maxillary prominences (Fig. 2Q). The frontonasal prominence remained free of X-Gal staining, in contrast to the strong staining in the lateral regions of the face (Fig. 2R,S). The size of the prominences, however, changes dramatically at this stage: in animals with muzzles or snouts, the rapid expansion of the maxillary and lateral nasal prominences relative to the slower growth of the frontonasal prominence results in compression of the frontonasal and in doing so, creates a furrow in the midline of the

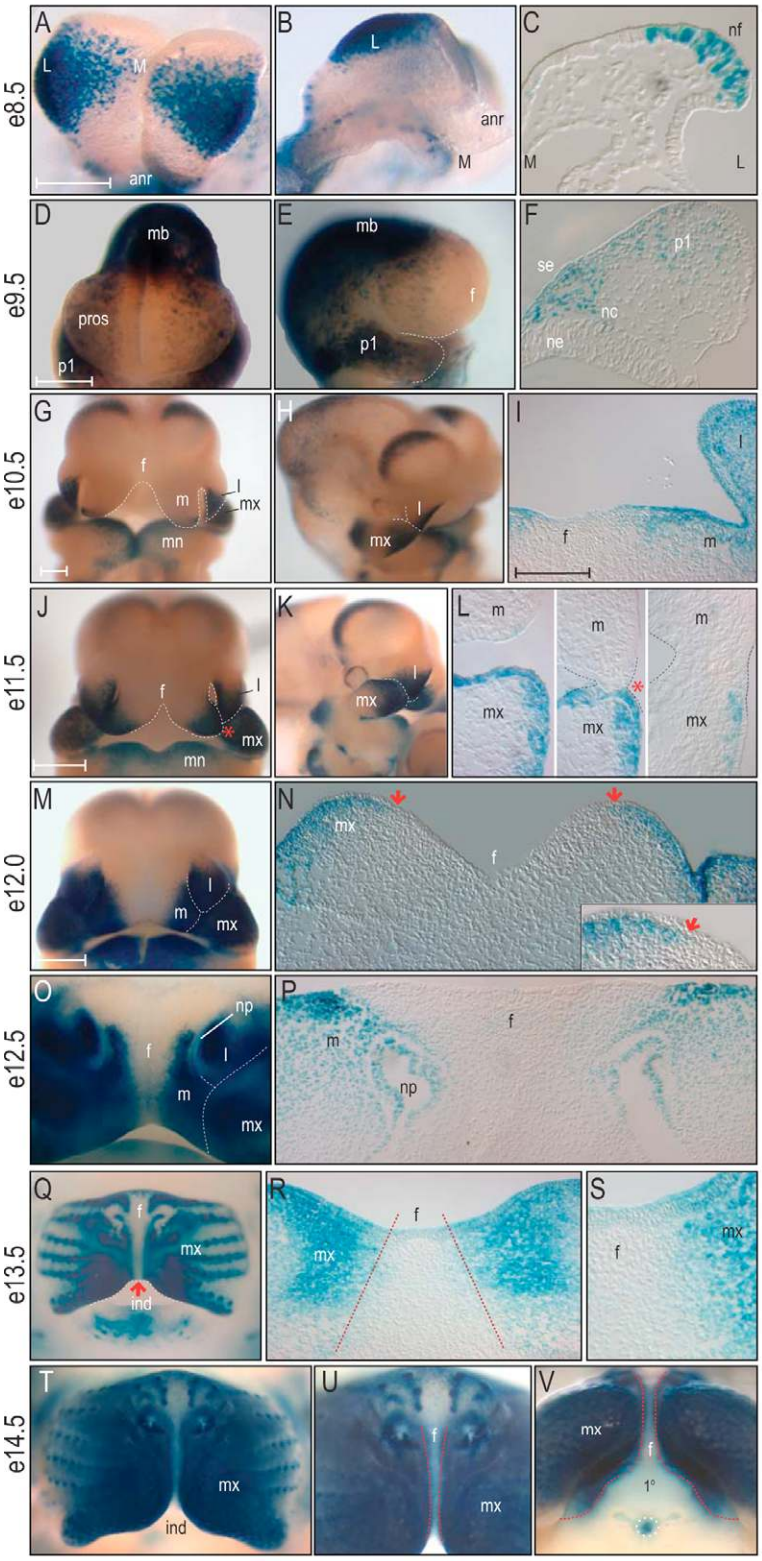

Fig. 2. Mapping the spatiotemporal pattern of β-gal activity in TOPgal Wnt reporter embryos. (**A**,**B**) At E8.5, reporter activity is restricted to the lateral (L) neural folds and is absent from the medial (M) midline region near the anterior neural ridge (anr). (**C**) X-Gal staining of a transverse section reveals reporter activity is confined to lateral neuroectoderm of the neural fold (nf). (**D**) Frontal and (**E**) lateral views at E9.5 illustrate reporter activity in cranial neural crest cells migrating into the first pharyngeal arch (p1) and the prosencephalon (pros). Cranial neural crest cells covering the midbrain (mb) are also β-gal-positive. (**F**) A transverse section through p1 show that at this stage, X-Gal staining is found in neural crest (nc) cells but not surface ectoderm (se) or neuroectoderm (ne). (**G**) Frontal and (**H**) lateral views at E10.5 indicate a distinct boundary between reporter-positive and reporter-negative cells. The frontonasal prominence (f) is devoid of staining, whereas some staining is evident in the median nasal prominence (m). The lateral nasal (l) and maxillary (mx) prominences show strong X-Gal staining. (**I**) Transverse sections reveal that surface ectoderm and mesenchyme of the median (m) and lateral nasal (l) prominences are sites of X-Gal staining, but neither surface ectoderm or mesenchyme in the frontonasal (f) prominence is positive for the reporter. (**J**) Frontal and (**K**) lateral views at E11.5 show an increase in X-Gal staining in the median nasal (m) prominence, whereas the frontonasal (f) prominence remains devoid of staining. At this stage, the median nasal prominence and maxillary prominence have fused (red asterisk). (**L**) Transverse sections show X-Gal staining disappears from surface ectoderm, but persists in maxillary mesenchyme as the prominences fuse (red asterisk). (**M**) Although reduced in size, the median nasal prominence remains free of X-Gal staining. (**N**) Transverse sections show a boundary between β-gal-positive and β-gal-negative regions in the frontonasal mesenchyme (red arrows). At this stage, X-Gal staining is restricted to mesenchyme (inset, red arrow). (**O**) At E12.5, the frontonasal (f) prominence is compressed by the growth of the maxillary (mx) prominences and (**P**) transverse sections show that the frontonasal region lacks reporter activity. The median nasal (m) prominence exhibits reporter activity. (**Q**) At E13.5, the mouse muzzle is fully formed and β-gal activity is evident in the whisker primordia. The continued growth of the maxillae (mx) relative to the compressed frontonasal (f) prominence produces the infranasal depression (ind, red arrow). (**R**,**S**) Transverse sections show the general lack of X-Gal staining in the frontonasal prominence relative to strong X-Gal staining in the maxillary prominences (mx, red dotted line). (**T**,**U**) Low- and high-power magnifications at E14.5 reveal frontonasal (f) prominence-derived tissues are reduced to a thin stripe of midline tissue (dotted red line) that generally maintains its β-gal-negative status. The maxillary prominences (mx) remain β-gal-positive. (**V**) A ventral view reveals the general lack of X-Gal staining in frontonasal prominence-derived primary (1°) palate. The boundary of X-Gal staining follows the demarcation between structures derived from the maxillary and frontonasal prominences (dotted red lines). White dotted circle, incisive foramen. Scale bars: white, 250 μm; black, 100 μm.

mouse face called the infranasal depression (Young et al., 2007). The infranasal depression remained conspicuously clear of reporter activity.

By E14.5, the muzzle of the mouse is fully formed and the frontonasal prominence is reduced to a thin sliver of midline tissue, sandwiched between the expanded maxillary prominences. The frontonasal-derived midline region still showed no evidence of X-Gal staining (Fig. 2T,U). When the embryo was rotated in order to view the palatal surface, the frontonasal prominence-derived primary palate was devoid of X-Gal staining (Fig. 2V). Collectively, these analyses in Wnt reporter embryos revealed a border between Wnt-responsive and non-responsive cells, which later distinguished the frontonasal prominence from the rest of the facial prominences.

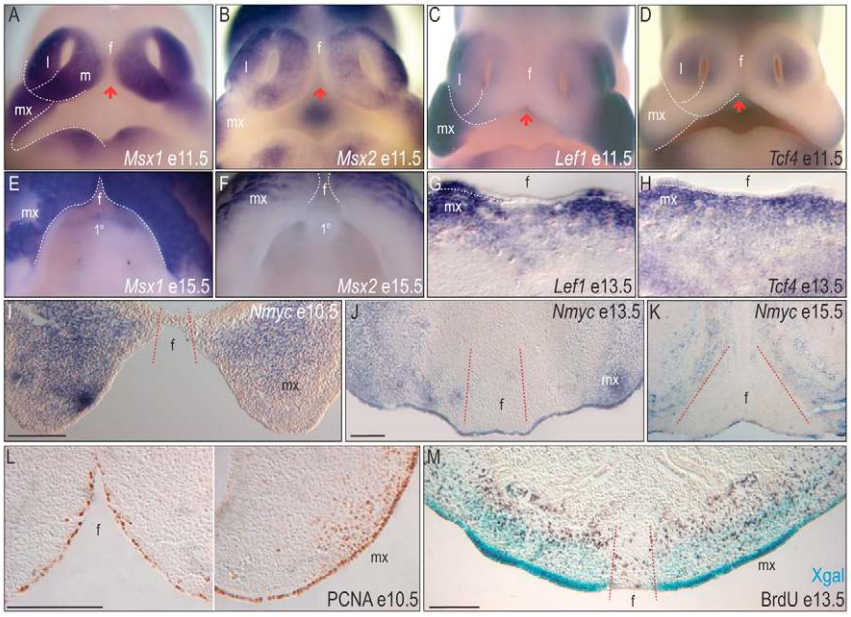

Fig. 3. Between E10.5 and E15.0, the expression of downstream targets and mediators of Wnt signaling correlates with sites of Wnt reporter activity. (**A**) At E11.5, *Msx1* is robustly expressed throughout the mouse maxillary (mx), lateral (l) and median (m) nasal prominences, whereas the frontonasal (f) prominence lacks *Msx1* expression (red arrow). (**B**) At E11.5, *Msx2* is also expressed in the maxillary (mx), lateral (l) and median (m) nasal prominences but is absent from the frontonasal (f) prominence (red arrow). (**C**) At E11.5, *Lef1* is expressed in the maxillary (mx) and, to a lesser extent, in the lateral nasal (l) prominences. Expression is largely absent from the frontonasal (f) prominence (red arrow). (**D**) *Tcf4* expression is confined to domains within the lateral (l) and median nasal (m) prominences, whereas the frontonasal (f) lacks *Tcf4* expression (red arrow). (**E**,**F**) Ventral view at E15.5 shows *Msx1* and *Msx2* expression limited to the maxillary (mx) prominences (dotted white line) and absent from frontonasal (f) prominence and the primary (1°) palate. (**G**) At E13.5, *Lef1* transcripts are detected in mesenchyme and ectoderm of the maxillary (mx) prominences, and at lower levels in frontonasal (f) mesenchyme. (**H**) *Tcf4* transcripts are evident through the frontonasal (f) and maxillary (mx) mesenchyme. (**I**) At E10.5, *Nmyc* transcripts localize to maxillary (mx) mesenchyme and are largely absent from frontonasal (f) tissues (red dotted line). (**J**) At E13.5, *Nmyc* is expressed in all surface ectoderm and continues to be expressed in maxillary mesenchyme (mx) but is absent from frontonasal (f) mesenchyme (red dotted line). (**K**) At E15.5, *Nmyc* maintains its same general expression pattern (red dotted line). (**L**) At E10.5, PCNA immunostaining on transverse sections shows evidence of cell proliferation in frontonasal (f) ectoderm and maxillary (mx) mesenchyme. (**M**) Co-staining for BrdU and β-gal shows that at E13.5, cell proliferation and reporter activity are colocalized to maxillary (mx) mesenchyme, whereas decreased levels of cell proliferation and reporter activity are detected in frontonasal (f) mesenchyme (dotted red line). Scale bars: 100 μm.

A Wnt-responsive boundary delineates the facial prominences

The patterns of β-gal reporter activity shown in Figs 1 and 2 suggest locations of Wnt responsiveness in the developing face. To verify that these were sites of Wnt signaling, we compared the X-Gal staining patterns with expression domains of genes that have been identified as Wnt targets in other tissues. For example, *Msx1* and *Msx2* are direct targets of Wnt signaling in embryonic carcinoma cells (Willert et al., 2002) and both transcription factors are involved in craniofacial patterning events (Foerst-Potts and Sadler, 1997; Levi et al., 2006; Satokata et al., 2000). Although their pattern of expression was not identical to that of reporter activity in TOPgal embryos, we found that at ~E11.5-12.5, the expression domains of Msx transcription factors mirrored the X-Gal staining patterns in two respects. First, neither gene was expressed in the frontonasal midline (Fig. 3A, arrows). Second, both genes were strongly expressed in the maxillary and lateral nasal prominences (Fig. 3A,B). At E15.5, we also noted that *Msx1* and *Msx2* were both excluded from derivatives of the frontonasal prominence (Fig. 3E,F), similar to the pattern of X-Gal staining we had observed in E15.5 TOPgal embryos (Fig. 2V).

We also found that a nuclear mediator of Wnt signaling, *Lef1*, was strongly expressed in the maxillary and lateral nasal prominences at E11.5 (Fig. 3C), whereas another mediator, *Tcf4*, was only expressed in mesenchyme surrounding the nasal pits (Fig. 3D). As with the Msx transcription factors, neither gene was expressed in the frontonasal midline (Fig. 3C,D, arrows). In older embryos, *Lef1* and *Tcf4* showed a more generalized pattern of expression in facial mesenchyme (Fig. 3G,H).

Nmyc (also known as *Mycn* – Mouse Genome Informatics) has been identified as a direct Wnt target by microarray screening (Nusse, 1999) and at early stages of development when the entire craniofacial complex is rapidly expanding, *Nmyc* is expressed throughout the craniofacial complex (data not shown). But as the facial prominences become progressively defined with age, we found that *Nmyc* expression was generally stronger in more lateral regions of the face and weaker in the frontonasal midline (Fig. 3I-K). In many tissues, *Nmyc* regulates cell proliferation (Hatton et al., 1996; Hirvonen et al., 1990; Mugrauer et al., 1988; Oliver et al., 2003; Zimmerman et al., 1986), so we next compared this pattern of cell proliferation with the pattern of *Nmyc* expression and Wnt reporter activity.

We found fewer PCNA-labeled cells in the E10.5 frontonasal prominence than in the adjacent maxillary prominences (Fig. 3L), which coincided with the compressed frontonasal midline and rapidly expanding lateral regions of the face. BrdU labeling experiments also showed generally greater labeling in the maxillary prominences compared with the frontonasal (Fig. 3M). The colocalization of Wnt reporter activity, Wnt target gene expression and cell proliferation was transient however; after E15.5, we could not detect similar relationships between X-Gal staining, gene expression and cell proliferation (data not shown). This suggested that the molecular boundary of Wnt responsiveness had transient significance for facial development. We set out to uncover what its possible function might be in regulating craniofacial morphogenesis.

A Wnt boundary in the face has functional significance

Thus far, our data indicated that beginning at ~E10.5 and continuing until E15.0, the frontonasal midline was a region of diminished Wnt responsiveness, and lateral regions of the face were sites of heightened Wnt responsiveness. To gain some insights into the possible function of Wnt signaling during this period of facial

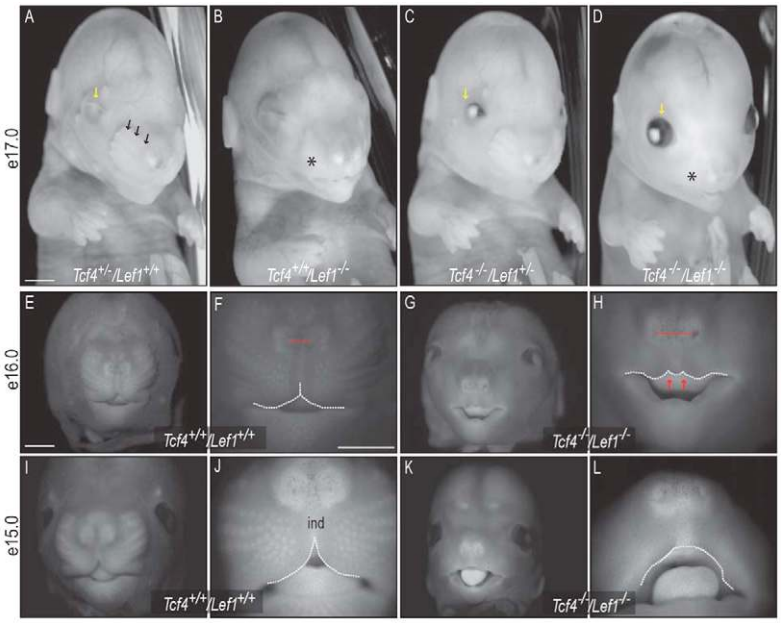

Fig. 4. *Tcf4*$^{-/-}$; *Lef1*$^{-/-}$ mutant mice have disrupted midfacial development and malformed teeth and tastebuds. (**A-D**) Whole-mount view of E17.0 embryos with varying dosages of *Tcf4* and *Lef1*. (A) *Tcf4* heterozygote embryos (*Tcf4*$^{+/-}$/*Lef1*$^{+/+}$) are unaffected, and epithelial specializations such as whiskers are present (black arrows), and eyelid fusion occurs normally (yellow arrow). (B) *Tcf4*$^{+/+}$; *Lef1*$^{-/-}$ mutants have disrupted whisker pattern (asterisk) and exhibit hypoplastic maxillae. (C) *Tcf4*$^{-/-}$; *Lef1*$^{+/-}$ mutants lack eyelids (yellow arrow). (D) *Tcf4*$^{-/-}$; *Lef1*$^{-/-}$ embryos show evidence of a severely reduced maxillae, in addition to their lack of eyelids and disrupted whisker primordia (yellow arrow and black asterisk). (**E-H**) In a comparison of E16.0 wild type and *Tcf4*$^{-/-}$; *Lef1*$^{-/-}$ compound mutants, wild-type embryos (E,F) show fully developed maxillae, an infranasal depression (dotted white line), and correctly spaced nostrils (dotted red line). Note organized whisker primordia. By contrast, *Tcf4*$^{-/-}$; *Lef1*$^{-/-}$ embryos (G,H) have a malformed frontonasal prominence and underdeveloped maxillae, which results in an infranasal depression that looks more like a human philtrum (dotted white line, red arrows). The nostrils are displaced laterally as a consequence (dotted red line). Note disorganized whisker primordia and absence of fused eyelids. (**I-L**) In a comparison of E15.0 wild-type and *Tcf4*$^{-/-}$; *Lef1*$^{-/-}$ embryos, wild-type embryos (I,J) show fully developed maxillae and organized whisker primordia; the infranasal depression (white dotted line, ind) is evident. *Tcf4*$^{-/-}$; *Lef1*$^{-/-}$ embryos (K,L) exhibit hypoplastic maxillae and lack the infranasal depression (dotted white line); note the absence of whisker primordia. Scale bar: 1 mm.

development, we initially pursued a genetic strategy. Disruptions in *Lef1* and *Tcf4* reduce the responsiveness of cells to Wnt signaling (DasGupta and Fuchs, 1999; DasGupta et al., 2002; Eastman and Grosschedl, 1999; Hussein et al., 2003; Reya et al., 2003) and yet, because of apparent redundancy in their function, embryos survive to birth (van Genderen et al., 1994). Thus, we could examine various combinations of *Tcf4* and *Lef1* heterozygous and homozygous embryos for changes in their facial appearances, all the while recognizing that these embryos are likely to represent a reduction rather than an elimination of Wnt signaling.

Tcf4$^{+/-}$; *Lef1*$^{+/+}$ heterozygotes exhibited no discernable craniofacial phenotypes (Fig. 4A), whereas *Tcf4*$^{-/-}$; *Lef1*$^{+/-}$ heterozygotes showed evidence of a disruption in whisker development (Fig. 4B, asterisk). The general morphology of the *Tcf4*$^{-/-}$; *Lef1*$^{+/-}$ face, however, was unperturbed. *Tcf4*$^{-/-}$; *Lef1*$^{+/-}$ embryos failed to completely fuse their eyelids (Fig. 4C, yellow arrow) but, once again, facial anatomy remained normal. Teeth, taste buds, whiskers and eyelids form as the result of Wnt-dependent interactions between facial ectoderm and neural crest-derived mesenchyme (Dassule and McMahon, 1998; Liu et al., 2003; Okubo et al., 2006; Ridanpaa et al., 2001; van Genderen et al., 1994) and the details of some of these aberrant epithelial-mesenchymal interactions have been reported by other groups (Sasaki et al., 2005; van Genderen et al., 1994) and us (Cadigan and Nusse, 1997; Korinek et al., 1998a; Korinek et al., 1998b) (D.t.B., J.A.H. and R.N., unpublished). Here, our focus was on how Wnt signaling regulated facial morphology, so we turned to the compound null homozygotes and examined their faces in more detail.

In sharp contrast to the single or compound heterozygotes, we found that *Tcf4*$^{-/-}$; *Lef1*$^{-/-}$ embryos exhibited radically altered faces (Fig. 4D). Upon careful comparison with their heterozygote and wild-type littermates, it became obvious that E17.0 *Tcf4*$^{-/-}$; *Lef1*$^{-/-}$ mutants had wide-set eyes and wide-set nostrils, i.e. a hyperteloric phenotype (Fig. 4D). Hypertelorism can result from an underlying brain abnormality, or from a disruption in facial patterning that is independent of a brain defect (Cordero et al., 2004; Cordero et al., 2005). We found no evidence of forebrain anomalies in the *Tcf4*$^{-/-}$; *Lef1*$^{-/-}$ mutants, so we concentrated on understanding the facial phenotype and determining when during development the malformation was first evident.

We found that at E16.0 the widened midface distinguished *Tcf4*$^{-/-}$; *Lef1*$^{-/-}$ mutants from their wild-type littermates (Fig. 4E,F compared with G,H; arrows and dotted lines). At still earlier stages (E15.0 and E15.5), wild-type embryos exhibited the characteristic infranasal depression and well-developed maxillae (Fig. 4I,J), whereas the *Tcf4*$^{-/-}$; *Lef1*$^{-/-}$ mutants had a flattened midline that blended into the poorly developed maxillae (Fig. 4K,L). At earlier stages (E14.0), the facial phenotype was no longer discernable. Therefore, our subsequent analyses concentrated on that developmental window when the *Tcf4*$^{-/-}$; *Lef1*$^{-/-}$ facial phenotype was first identifiable.

In E15.0 wild-type and heterozygous embryos, the nasal septum is an elongated, cartilaginous rod that extends into the muzzle of the mouse (Fig. 5A). The nasal septum is contiguous with the nasal capsule, which encompasses the nasal epithelium and forms within the frontonasal prominence (Fig. 5B). In *Tcf4*$^{-/-}$; *Lef1*$^{-/-}$ embryos, the nasal septum and capsule were severely truncated (Fig. 5C,D). The length of the *Tcf4*$^{-/-}$; *Lef1*$^{-/-}$ nasal septum was reduced by over 52%, and the mediolateral width of the frontonasal prominence was increased by over 25% (Fig. 5, compare A with D, and B with C). This malformation was largely confined to the frontonasal prominence; the position and orientation of the basisphenoid, the palatal process of the palatine and the palatal process of the maxilla, the basal plate, and the trabecular plate of the nasal septum were relatively unaffected by the loss of Lef1 and Tcf4 (Fig. 5E,F).

In keeping with the well-known function of Wnt signaling in tooth morphogenesis, we found evidence of odontogenic defects in *Tcf4*$^{-/-}$; *Lef1*$^{-/-}$ embryos. Specifically, the dental epithelium showed evidence of thickening and invagination, and the underlying dental mesenchyme had undergone condensation, but further development

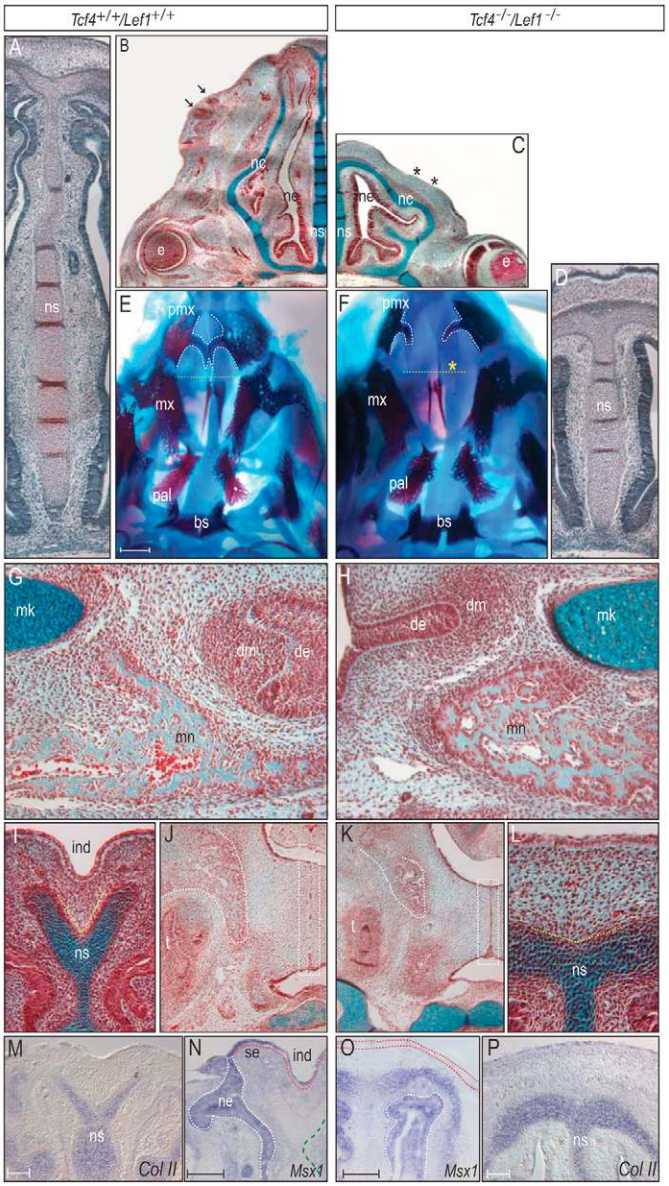

Fig. 5. Skeletal and molecular analyses of *Tcf4*$^{-/-}$; *Lef1*$^{-/-}$ compound mutants. Histological staining on transverse sections through E15.5 wild-type (*Tcf4*$^{+/+}$/*Lef1*$^{+/+}$) mouse embryos shows (**A**) the normal length of the cartilaginous nasal septum (ns) and (**B**) the curvature of the nasal cartilage (nc) and condensations of the whisker buds (black arrows). The nasal epithelium (ne) is correctly organized. (**C**) In compound null-mutant embryos nasal cartilage (nc) growth is truncated and whisker buds are absent (black asterisks). Despite this dramatic alteration in shape, the cartilage is still well developed and the nasal epithelium (ne) is organized. (**D**) In contrast to the wild-type nasal septum shown in A, the mutant nasal septum is dramatically foreshortened. (**E**,**F**) Ventral view of Alcian Blue/Alizarin Red skeletal preparation (mandibles removed) shows that in wild-type embryos (E), the basisphenoid (bs), premaxillae (pmx, white dotted line), maxillae (mx), palatine bones (pal) and the nasal septum have formed normally and have their proper orientation relative to one another. (F) *Tcf4*$^{-/-}$; *Lef1*$^{-/-}$ mutants exhibit grossly underdeveloped premaxillae (pmx, dotted white line), which fail to make contact and fuse across the midline. The major skeletal elements of the posterior palate appear normal. (**G**) Pentachrome staining of transverse sections through E15.5 jaws reveal tooth primordia at the bell stage, where the dental epithelium (de) has invaginated and dental mesenchyme (dm) has condensed in response to signals from the ectoderm. (**H**) *Tcf4*$^{-/-}$; *Lef1*$^{-/-}$ dental epithelium (de) fails to invaginate properly. Note, however, that maturation of Meckel's cartilage (mk) and the bone of the mandible (mn) are unaffected by the loss of Tcf4 and Lef1. (**I**,**J**) Pentachrome staining of transverse sections through E15.5 wild-type embryos reveals the characteristic 'Y' shape (yellow dotted line) of the anterior nasal septum, which correlates to the location of the infranasal depression (ind). In an adjacent tissue section, the osteogenic condensation of the maxillae is evident (dotted white line), as well as the tooth (t) and epithelial seam (dotted white box) of the palatal shelves, which is dissolving on an appropriate time scale. (**K**,**L**) In E15.5 *Tcf4*$^{-/-}$; *Lef1*$^{-/-}$ littermates, the osteogenic condensation of the maxillae is reduced (dotted white line), the tooth (t) is developmentally delayed and the epithelial seam (dotted white box) of the palatal shelves remains evident. The anterior nasal septum exhibits a dysmorphic 'T' shape (yellow dotted line), corresponding to the malformed midface seen earlier (Fig. 4). (**M**,**N**) In situ hybridization on transverse sections of E15.5 wild-type embryos shows that collagen II (*Col II*) is expressed throughout the cartilaginous nasal septum (ns) and *Msx1* transcripts are detected in surface ectoderm (se, dotted red line), nasal epithelium (ne) and undifferentiated mesenchyme. (**O**,**P**) In E15.5 *Tcf4*$^{-/-}$; *Lef1*$^{-/-}$ littermates, *Msx1* expression is specifically lost in surface ectoderm (dotted red line) but maintained in nasal epithelium and underlying mesenchyme. Collagen II transcripts persist in the dysmorphic nasal septum (ns), indicating normal chondrocyte differentiation. Scale bars: white, 1 mm; black, 100 μm.

of the tooth primordia beyond the cap stage was arrested (Fig. 5G,H). Details of this odontogenic defect will be described elsewhere.

In the same tissue section we found a dramatic example of the specificity of the *Tcf4*$^{-/-}$; *Lef1*$^{-/-}$ defect: although the morphology of facial skeletal elements was severely disrupted, the programs of chondrogenesis and osteogenesis were unimpeded (Fig. 5G,H). This is especially interesting because of the documented role of Wnt signaling in regulating both skeletal programs in long bones (Day et al., 2005; Hu et al., 2005; Kolpakova and Olsen, 2005) (reviewed by Hartmann, 2006).

We returned to study in more detail the morphology of the *Tcf4*$^{-/-}$; *Lef1*$^{-/-}$ frontonasal prominence, which exhibited the most obvious defect. In wild-type embryos, the distal-most tip the nasal septum branches into a 'Y' shape to accommodate the maxillary-derived portion of the muzzle (Fig. 5I). In the *Tcf4*$^{-/-}$; *Lef1*$^{-/-}$ mutants, the nasal septum adopted a 'T' shape (Fig. 5L). At E15.0, the palatal shelves had fused and the intervening epithelium was in the process of being removed (Fig. 5K). In *Tcf4*$^{-/-}$; *Lef1*$^{-/-}$ mutants, the shorter palatal shelves also fused, but we routinely detected residual epithelial rests remaining in the seam area (n=3; Fig. 5L). The skeletal abnormalities we found in the frontonasal prominence-derived structures were not associated with a disruption in chondrogenesis, as shown by the persistence of collagen type II (Fig. 5, compare M with P), but they were accompanied by the selective loss of *Msx1* expression in surface ectoderm (Fig. 5, compare N with O; dotted red lines). *Msx1* continued to be expressed in nasal epithelium and in the undifferentiated mesenchyme.

These molecular and cellular analyses indicated that the combined loss of *Tcf4* and *Lef1*, which results in a loss of Wnt signaling (Reya et al., 2003) (4948), dramatically altered facial morphology. This dysmorphology was not the result of perturbed

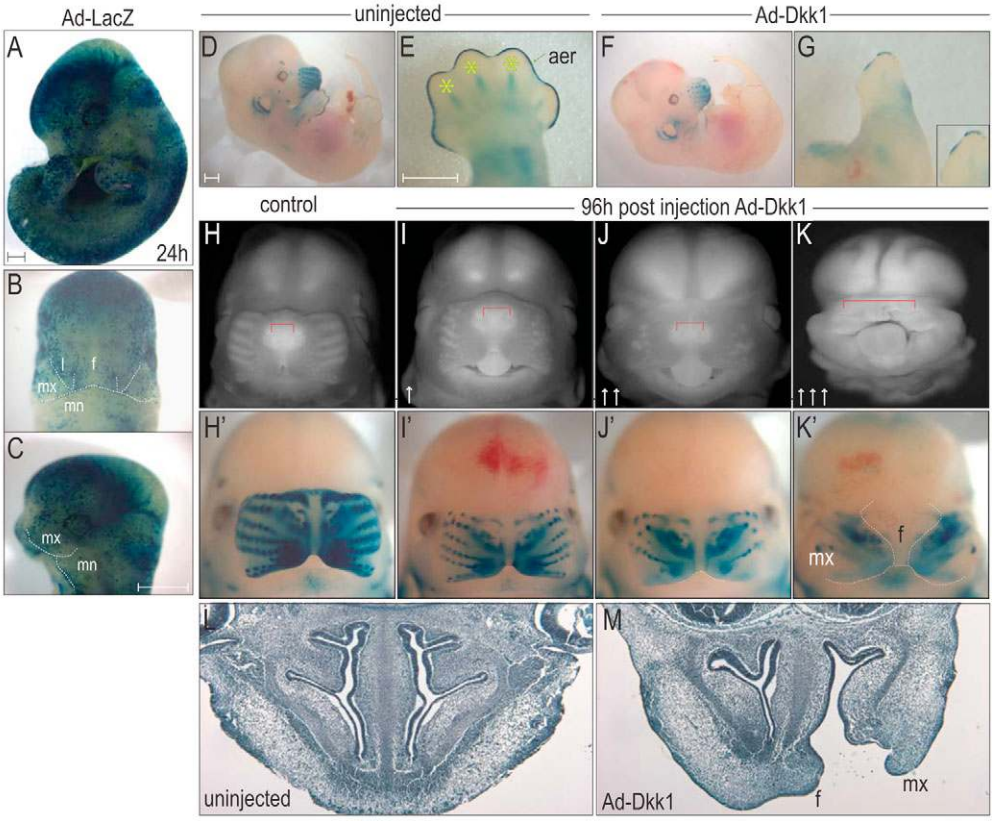

Fig. 6. In utero gene transfer of a Wnt inhibitor phenocopies the *Tcf4*$^{-/-}$; *Lef1*$^{-/-}$ facial defect. (**A-C**) Mouse embryos were injected at E10.5 with a control adenovirus encoding *lacZ* then collected 24 hours later and stained for β-gal activity. Lateral and frontal views show widespread X-Gal staining, indicating widespread, unifrom adenoviral infection in the lateral nasal (l), frontonasal (f), maxillary (mx) and mandibular (mn) prominences. (**D**,**E**) Non-injected or (**F**,**G**) Ad-Dkk1-injected embryos were collected at E13.5 (i.e. 96 hours after injection at E9.5). (D,E) Control embryos show characteristic Wnt reporter activity in the face and limb buds; note activity in the apical ectodermal ridge (aer) and skeletal condensations of the forelimb (yellow asterisks). (F,G) Ad-Dkk1 treatment truncates Wnt-dependent forelimb and digit growth (inset); note corresponding reduction in Wnt reporter activity. (**H-K′**) Comparison between control and Ad-Dkk1-treated faces. (H,H′) Control embryos exhibit normal facial morphology and undisturbed boundaries of Wnt reporter activity in the face and whisker buds. (I-K′) Ad-Dkk1-treated embryos show an increasingly severe facial malformation that parallels the reduction in Wnt reporter activity. For example, the width of the frontonasal prominence is variably expanded (compare red brackets) owing to a reduction in growth of the maxillae. The more severe phenotypes correspond to the most dramatic reduction in Wnt reporter activity, so that the maxillary (mx) prominences are smaller and the frontonasal (f) is concomitantly larger. The reduction in X-Gal staining is clearly visible in Ad-Dkk1-treated whisker primordia. (**L**,**M**) Transverse sections through embryos collected at E13.5 (96 hours after injection at E9.5). Control (L, non-injected) nasal capsules show normal fusion of the facial prominences. In Ad-Dkk1-treated embryos (M), the reduction in maxillary growth is sometimes associated with facial clefting. Scale bars: white, 1 mm; black, 500 μm.

differentiation of skeletal tissues. Rather, the defect stemmed from a disruption in localized, Wnt-mediated expansion of the maxillary prominences and a concomitant contraction in the frontonasal prominence (Fig. 4). Together, these morphogenetic forces adversely affected the shape and relative positions of frontonasal and maxillary-derived skeletal elements (Fig. 5).

Inhibiting Wnt signaling in utero phenocopies *Lef1*$^{-/-}$; *Tcf4*$^{-/-}$ mutant phenotype

Using *Lef1*$^{-/-}$; *Tcf4*$^{-/-}$ mutants was one mechanism to assess the role of Wnt signaling during craniofacial morphogenesis. We also employed another approach, in which Wnt signaling was downregulated in utero by overexpressing the soluble Wnt inhibitor Dkk1 (Hoffman et al., 2004). We used this alternative strategy because we wanted to exclude the possibility that the *Lef1*$^{-/-}$; *Tcf4*$^{-/-}$ facial phenotype was attributable to a disruption in cranial neural crest cell generation and/or migration. Since both of these processes are affected by Wnt signaling (Burstyn-Cohen et al., 2004; De Calisto et al., 2005; Garcia-Castro et al., 2002) we opted to block Wnt signaling after cranial neural crest cells had migrated into the facial prominences, at ~E9.5 (Osumi-Yamashita et al., 1994; Osumi-Yamashita et al., 1997). We injected adenovirus expressing Dkk1 (Ad-Dkk1) into individual uteri of TOPgal dams at E9.5 and harvested the embryos at E13.5 for analysis. As a control, we injected Ad-*lacZ* to ascertain the approximate level of expression that was achieved within 24 hours of viral delivery. Control Ad-*lacZ* embryos showed abundant, widespread staining throughout the surface ectoderm in a roughly uniform pattern (Fig. 6A). Of particular interest was the pattern of reporter activity in the facial prominences: all facial ectoderm appeared to be similarly affected by the adenoviral infection (Fig. 6B,C). Therefore, this delivery method could serve as a reasonable proxy for inhibiting Wnt signaling from facial ectoderm, and we could be fairly certain of widespread infection within 24 hours of injection.

In our next experiments, E9.5 embryos were infected with Ad-Dkk1 and then harvested 96 hours later. First, we found no differences in the size of control and Ad-Dkk1-treated embryos (Fig. 6, compare D with F), which indicated that Ad-Dkk1 infection did not cause a generalized growth arrest. Second, because we used TOPgal embryos for this experiment we could gauge the level of Wnt inhibition by assessing the extent of X-Gal staining. For example, we found that some regions, such as the limb bud, were particularly sensitive to Wnt inhibition. Wnt signaling from the apical ectodermal ridge regulates limb outgrowth (Kengaku et al., 1998) and we found that Ad-Dkk1 completely disrupted this event (Fig. 6, compare E with G). In addition, Wnt signaling influences the growth of chondrogenic condensations in the E12.0 limb (Hartmann and Tabin, 2000) and this process was also perturbed by Ad-Dkk1 infection (Fig. 6E,G). These results confirmed that Ad-Dkk1 infection selectively blocked Wnt-mediated developmental

events that were initiated sometime after the stage of infection, ~E9.5. They also demonstrated that X-Gal staining in TOPgal embryos was a reliable readout of endogenous Wnt signaling, and that a reduction in X-Gal staining was an accurate demonstration of reduced Wnt signaling. Regarding this latter point, we found that Ad-Dkk1 treatment routinely led to a reduction in X-Gal staining, which was especially notable in the whisker primordia (compare control, Fig. 6H′ with 6I′-K′).

Of particular interest were the consequences of Ad-Dkk1 treatment on facial development: in the majority of cases (40/65), Ad-Dkk1 resulted in a severe reduction of the maxillary prominences and an accompanying expansion of the frontonasal prominence (Fig. 6, compare H,H′ with I-K). The phenotypes ranged in severity from a subtle change to a profound alteration in mediolateral width of the face (Fig. 6I-K′). In the most severe cases (~4%), the facial malformation was accompanied by a cleft between the frontonasal and maxillary prominences (Fig. 6, compare L with M). This was a rare occurrence, however, because facial fusions begin around the time we delivered the adenovirus. When considered along with the *Lef1; Tcf4*-null phenotype, we conclude that two complementary methods, both of which disrupted Wnt signaling, produced the same facial phenotype: a flattened mouse midface that lacked its characteristic infranasal depression.

Wnt signaling regulates differential growth of the facial prominences

Thus far our data demonstrate that Wnt signaling appears to support cell proliferation and, as a consequence, Wnt-responsive maxillary-derived regions of the mouse face expand. The frontonasal ectoderm lacks Wnt responsiveness and thus this region of the face does not show the same degree of cell proliferation. When maxillary expansion of the prominences is coupled to reduced frontonasal growth, the resulting face has a midline furrow and enlarged maxillae that form the snout, or muzzle. Our analyses of $Tcf4^{-/-}$; $Lef1^{-/-}$ and Ad-Dkk1 embryos indicate that Wnt signaling is a mediator of differential growth in the face. We sought to validate this conclusion in other animal taxa and therefore turned to an animal whose facial morphology is the antithesis of the mouse.

In birds, the frontonasal prominence forms a protrusion rather than a furrow (Fig. 7, compare A with B). The maxillary prominences, on the other hand, do not expand to nearly the same degree as they do in the mouse, the net result being an elongated beak. If Wnt signaling is a conserved mechanism whereby facial diversity is created, we hypothesized that Wnt signaling in the bird face would be the reverse of what we observed in mice: namely, the frontonasal midline would show an increase in Wnt signaling, whereas the maxillary prominences would be sites of diminished Wnt signaling.

In order to examine Wnt responsiveness in an avian model we generated a viral Wnt reporter construct. In our avian reporter construct, GFP is expressed under the control of seven Tcf-binding sites (pLenti 7xTcf-eGFP). This construct is similar to the reporter construct in TOPgal mice used in our initial experiments (Fig. 2) (DasGupta and Fuchs, 1999), the exception being the number of Tcf-binding sites (seven in our GFP virus versus three in TOPgal embryos). Although this difference in the number of binding sites might affect the sensitivity of one construct in comparison to another (Barolo, 2006), both reporters are activated only when cells are presented with a Wnt ligand, which we demonstrated by testing the activity of the 7xTcf-eGFP construct in vitro. We infected murine adipose-derived mesenchymal cells and then exposed them 48 hours

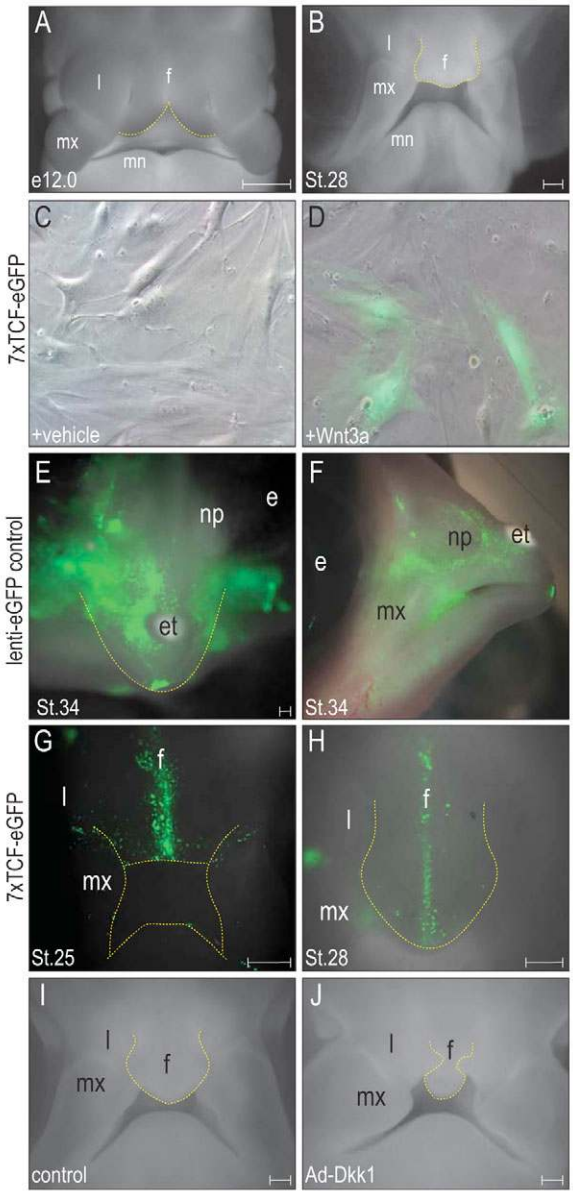

Fig. 7. Wnt responsiveness predicts differential growth of the facial prominences. (**A**) In the E12.0 mouse face, growth of the frontonasal prominence relative to the lateral nasal (l) and maxillary (mx) prominences produces a midline furrow (dotted yellow line). (**B**) In chick, the converse is seen, where the frontonasal prominence grows at a faster rate than the maxillary and lateral nasal prominences, thus producing a pointed beak. (**C**,**D**) Adipose-derived mouse mesenchymal cells infected with a 7xTcf-eGFP lentivirus and incubated in control medium do not express the GFP reporter (C), but addition of purified Wnt3a protein activates GFP expression (D). (**E**,**F**) In chick, injection of a control lenti-eGFP at St. 13 results in widespread infection by St. 34. GFP expression is scattered throughout the upper beak; E, frontal view; F, lateral view. et, egg tooth; np, nasal pit; e, eye. (**G**) In chick, injection with 7xTcf-eGFP at St.13 results in a robust, spatially restricted pattern of GFP expression in the midline of the frontonasal prominence by St. 25. (**H**) At St. 29 in chick, this same pattern of GFP expression is seen in the frontonasal midline. (**I**,**J**) The frontonasal midline of avian embryos is a site of continued growth that eventually results in the elongated upper beak. When Wnt signaling is inhibited in avians by Ad-Dkk1 injection at St. 13, the growth of the frontonasal midline is dramatically impeded (compare dotted yellow line in I and J). The lateral nasal and maxillary prominences are unaffected. Scale bars: 250 μm.

later to either vehicle or purified Wnt3a protein. GFP activity was only detectable when cells were treated with Wnt3a (Fig. 7C,D). These data demonstrate that canonical Wnt signaling specifically activated GFP expression in cells infected with the 7xTcf-eGFP lentivirus.

We next examined Wnt responsiveness in chick in ovo by infecting embryos at stage (St.) 13 with pLenti 7xTcf-eGFP. We chose this time point because it is analogous to E9.5 in mice in that the majority of cranial neural crest cells destined for the frontonasal prominence are already in place but differential outgrowth of the prominences has yet to ensue. We performed one additional control experiment: to prove that lentiviral injection was a plausible mechanism to broadly infect the avian face, we injected a control lenti-eGFP virus at St. 13 and harvested embryos at St. 28. Injection of the control GFP virus resulted in a broad and extensive infection of the facial prominences (Fig. 7E,F), demonstrating that our injection technique was suitable for labeling the majority of cells in the facial prominences.

We then undertook our experiment to map reporter activity in the avian face. We injected pLenti 7xTcf-eGFP at St. 13 and then collected embryos 48 and 72 hours later. Contrary to the mouse, where Wnt reporter activity was robust in the maxillary and lateral nasal prominences and absent in the frontonasal prominence, the St. 25 chick exhibited a robust region of reporter activity in a midline stripe down the frontonasal prominence (Fig. 7G). By contrast, the maxillary and lateral nasal prominences showed no evidence of reporter activity (Fig. 7G). At St. 28, the pattern of reporter activity was the same: robust signal in the frontonasal midline and no discernable activity in the maxillary prominences (Fig. 7H). These results indicated that in avians, the midline of the frontonasal prominence is a region of Wnt reporter activity, whereas the lateral nasal and maxillary prominences are devoid of Wnt reporter activity. These findings are in keeping with the dramatically elongated frontonasal prominence in avians.

We also tested the consequences of reducing Wnt signaling during chick craniofacial morphogenesis. The previous results indicated that Ad-Dkk1 virus inhibited the growth of Wnt-responsive facial prominences. Here, we found that Ad-Dkk1 treatment resulted in embryonic death in ~45% of treated embryos, but of those that survived, 11% showed a dramatic and specific arrest in frontonasal outgrowth (n=68; Fig. 7I,J). We saw little to no change in outgrowth of the lateral nasal or maxillary prominences (Fig. 7I,J) which, as our reporter results indicated, were not sites of abundant Wnt signaling. When considered together, these avian data confirm that sites of endogenous Wnt signaling in the face show abundant growth, whereas sites lacking endogenous Wnt signaling show much less expansion. Consequently, the regional pattern of Wnt signaling influences the pattern of growth within the facial prominences by a mechanism that appears to be conserved between species.

DISCUSSION

One of the principal objectives of developmental biology is to understand morphogenesis and, in doing so, gain insights into the genetic basis of variation observed in the animal kingdom. Here, we studied how facial diversity is created. We used genetic and biochemical methods to first study and then perturb Wnt signaling in murine and avian embryos. As a consequence, we found clues as to how differential growth is regulated to achieve species-specific facial features.

We found that the facial prominences could be divided into domains of Wnt-responsive and non-responsive cells, and that these molecular boundaries later corresponded to discrete morphological structures. For example, in two strains of transgenic Wnt reporter embryos the frontonasal prominence was a reporter-negative domain and both the maxillary and lateral nasal prominences were reporter-positive regions. Later, the reporter-negative region precisely corresponded to derivatives of the frontonasal prominence, and the reporter-positive regions arose from the lateral nasal and maxillary prominences (Figs 1 and 2).

We also found that the territories of Wnt-responsive cells tended to show evidence of more cell proliferation, at least at the developmental stages we examined (Fig. 3). When Wnt signaling was perturbed, either through genetic activation of the *Tcf4*/*Lef1* nuclear mediators, or by overexpression of a soluble Wnt antagonist, then the distinctive facial features of the mouse were lost. The effect was primarily limited to the neural crest-derived facial skeleton and could most accurately be described as a transformation of sorts: the typical infranasal depression that is a characteristic of the muzzle-faced mouse was transformed into a flattened, smooth midface, reminiscent of the human midface.

Craniofacial growth is influenced by Wnt signaling

Wnt signaling has been implicated in a wide variety of developmental processes from cell proliferation to cell fate determination and differentiation, to cell survival (Cadigan and Nusse, 1997; Wodarz and Nusse, 1998). In craniofacial development, Wnt signaling has been most commonly linked to the generation and migration of neural crest cells. Many Wnt ligands and receptors continue to be expressed in the craniofacial complex well after the neural crest cells have completed their migration (Gavin et al., 1990; Oosterwegel et al., 1993; Wang and Shackleford, 1996), which begs the question: is there an additional role for Wnt signaling in the facial prominences after the birth and migration of neural crest cells?

Recent studies lend convincing evidence that this is the case. In humans, mutations in the *WNT3* gene are associated with tetra-amelia and cleft lip and palate (Niemann et al., 2004). The A/WySn strain of mice exhibits an increased incidence of cleft lip and palate, and recent data indicate that this increased incidence can be exacerbated still further by deleting *Wnt9b* (Juriloff et al., 2006). Here, our data indicate a novel role for Wnt signaling in regulating species-specific craniofacial morphogenesis.

Our data indicate that prior to outgrowth, Wnt responsiveness is conspicuously absent from the facial midline and is restricted to the lateral portions of the facial prominences. This boundary between Wnt-responsive and non-responsive regions is maintained as the individual prominences grow. We examined two of the five available transgenic reporter mice (DasGupta and Fuchs, 1999; Maretto et al., 2003; Moriyama et al., 2007; Yu et al., 2005) and found the same general pattern of reporter activity in this region of the head.

Although by no means exclusive, regions of strong Wnt responsiveness coincided with elevated cell proliferation. At some embryonic stages, Wnt responsiveness also coincided with the domains of *Nmyc* and *Msx1* expression. Both genes have been identified through microarray screens as Wnt targets in other cell types, but whether they represent Wnt targets in the face still remains to be determined. In the case of the Msx genes, some data suggest that they are targets of BMP signaling during odontogenesis (Tucker et al., 1998; Vainio et al., 1993), and there is a recognized interaction between BMP and Wnt signaling during neural crest induction (Garcia-Castro et al., 2002; Monsoro-Burq et al., 2005). Precisely how Wnt and BMP signaling are coordinated during facial morphogenesis is, however, still not known.

Wnt signaling is essential for regional specification of the face

We postulated that Wnt signaling is a crucial regulator of facial morphogenesis, and to test this hypothesis we used two complementary approaches to mitigate Wnt signaling. Two intracellular enhancers of Wnt signaling, *Lef1* and *Tcf4*, were deleted by homologous recombination and the result of this mutation was a reduction in Wnt signaling in the face. Although single heterozygotes had tooth, whisker and taste bud defects, they exhibited normal facial appearance. In sharp contrast, $Lef1^{-/-}$; $Tcf4^{-/-}$ mutants exhibited a foreshortened midface. Skeletal elements all formed but those derived from the frontonasal prominence were truncated and the midface was dramatically wider. We observed a very similar facial phenotype in mouse embryos exposed in utero to the Wnt inhibitor Dkk1 on E9.5. When considered together, these data indicate that Wnts act as molecular mediators of regional specification within the craniofacial prominences.

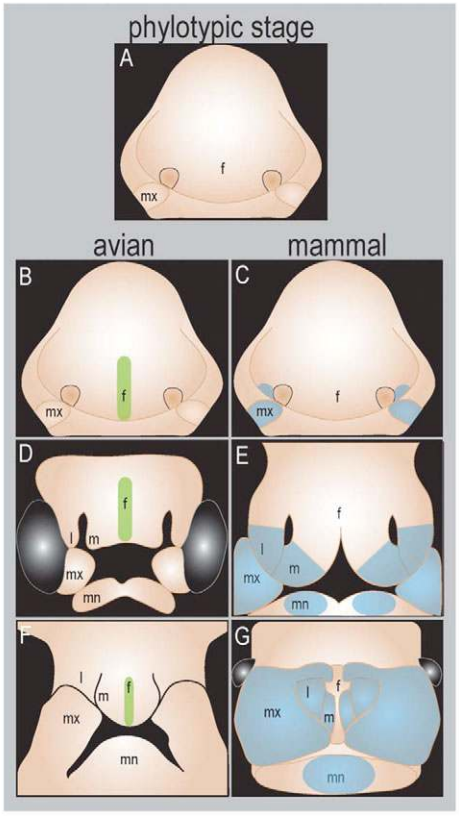

Fig. 8. Model of Wnt-mediated signaling regulating species-specific facial morphogenesis. (**A**) At the phylotypic stage of development, murine and avian embryos have very similar facial features. (**B**,**C**) Our data suggest that species-specific patterns of Wnt responsiveness pre-date and predict regional growth within the facial prominences. For example, in embryos with an elongated frontonasal prominence (B), Wnt responsiveness (green) predominates in the midline, whereas in embryos with a compressed frontonasal region and expanded maxillary prominences (C), Wnt signaling (blue) dominates in the lateral regions and is absent from the midline. (**D**,**E**) Wnt responsiveness is predictive of areas of greater outgrowth. In avians (D), Wnt signaling is dominant in the frontonasal midline but in animals with muzzles or snouts (E), Wnt signaling is largely confined to the expanding lateral facial prominences. (**F**,**G**) When the facial prominences have assumed their species-specific morphology, Wnt signaling is maintained in regions of outgrowth. In avians (F), this area correlates to the apex of the upper beak, whereas in mice (G) it correlates to the expanding maxillary prominences.

Morphometric studies show that in animals with muzzles, the rapid expansion of the maxillae restricts growth of the frontonasal prominence (Young et al., 2007), which results in a characteristic furrow called the infranasal depression. In humans, the infranasal depression corresponds to a vestigial philtrum, which is the small depression located between the base of the nostrils and the upper lip.

A critical reader might question why this region of facial anatomy garners such close consideration. As it turns out, differences in the organization of this region of the face are the distinguishing characteristic among a host of animals, most notably primates (Martin et al., 1996). The most prominent feature distinguishing two primates, stepsirhines and haplorhines, is their midface and nose (Hershkovitz, 1977). Stepsirhines have snouts, similar to mice, complete with an infranasal depression that separates the narrow nostrils. In haplorhines (monkeys, apes and humans), the midface lacks an infranasal depression and instead exhibits a vestigial philtrum. A similar distinction could be made between wild-type and $Tcf4^{-/-}$; $Lef1^{-/-}$ or Ad-Dkk1 embryos. In both of these mutants, the midface loses its characteristic snout-like appearance because of a lack of maxillary growth and a concomitant expansion in the frontonasal prominence. Consequently, the midface is flattened and smooth, without its infranasal depression, and instead adopts a philtrum-like anatomy.

The role of Wnts in differential growth is conserved across species

Our analysis of Wnt responsiveness in mice suggests that Wnts create molecular demarcations that predate changes in morphology of the facial prominences. Even before species-specific facial features are evident in murine embryos (E9.5), the patterns of Wnt reporter activity suggest a regional specification within the facial prominences. We found this regional specification by Wnt signaling is conserved in at least two model organisms. By creating an avian reporter virus we were able to assay Wnt responsiveness in a species that had a complementary pattern of facial outgrowth to the mouse. Whereas the frontonasal prominence of the mouse forms the infranasal depression and lacks any Wnt-responsive cells, the frontonasal prominence of the chick forms a prominent, protruding beak and, correspondingly, has a conspicuous streak of Wnt-responsive cells in its midline (Fig. 8). Contrary to the situation in mouse, the lateral nasal and maxillary prominences of chick do not display any evidence of reporter activity and, coincidentally, these prominences expand far less than the avian frontonasal prominence.

The results of this cross-species comparison of Wnt signaling in the face might carry profound evolutionary significance. A conserved mechanism of variations in Wnt signaling could account for the different facial appearance of all animals ranging from hammerhead sharks to anteaters. Detailing the extent of Wnt signaling in the developing facial primordia will be an important next step in our research.

We thank Dr Calvin Kuo of Stanford University for supplying Ad-Dkk1 virus and members of the Helms and Nusse laboratories for their helpful comments. This work was supported by MOD FY06-335 (J.A.H.), NRSA-F32DE017499-01 (S.A.B.), RO1-DE012462-06A1 (J.A.H.) and the Swiss National Science Foundation (C.F.).

References

Albrecht, U. E. G., Helms, J. A. and Lin, H. (1997). Visualization of gene expression patterns by in situ hybridization. In *Molecular and Cellular Methods in*

Developmental Toxicology (ed. G. P. Daston), pp. 23-48. Boca Raton, FL: CRC Press.
Barolo, S. (2006). Transgenic Wnt/TCF pathway reporters: all you need is Lef? *Oncogene* **25**, 7505-7511.
Brugmann, S. A., Kim, J. and Helms, J. A. (2006). Looking different: understanding diversity in facial form. *Am. J. Med. Genet. A* **140**, 2521-2529.
Burstyn-Cohen, T., Stanleigh, J., Sela-Donenfeld, D. and Kalcheim, C. (2004). Canonical Wnt activity regulates trunk neural crest delamination linking BMP/noggin signaling with G1/S transition. *Development* **131**, 5327-5339.
Cadigan, K. M. and Nusse, R. (1997). Wnt signaling: a common theme in animal development. *Genes Dev.* **11**, 3286-3305.
Cordero, D., Marcucio, R., Hu, D., Gaffield, W., Tapadia, M. and Helms, J. A. (2004). Temporal perturbations in sonic hedgehog signaling elicit the spectrum of holoprosencephaly phenotypes. *J. Clin. Invest.* **114**, 485-494.
Cordero, D., Tapadia, M. and Helms, J. A. (2005). *Sonic Hedgehog Signaling in Craniofacial Development*. Georgetown, TX: Eureka Biosciences.
DasGupta, R. and Fuchs, E. (1999). Multiple roles for activated LEF/TCF transcription complexes during hair follicle development and differentiation. *Development* **126**, 4557-4568.
DasGupta, R., Rhee, H. and Fuchs, E. (2002). A developmental conundrum: a stabilized form of beta-catenin lacking the transcriptional activation domain triggers features of hair cell fate in epidermal cells and epidermal cell fate in hair follicle cells. *J. Cell Biol.* **158**, 331-344.
Dassule, H. R. and McMahon, A. P. (1998). Analysis of epithelial-mesenchymal interactions in the initial morphogenesis of the mammalian tooth. *Dev. Biol.* **202**, 215-227.
Day, T. F., Guo, X., Garrett-Beal, L. and Yang, Y. (2005). Wnt/beta-catenin signaling in mesenchymal progenitors controls osteoblast and chondrocyte differentiation during vertebrate skeletogenesis. *Dev. Cell* **8**, 739-750.
De Calisto, J., Araya, C., Marchant, L., Riaz, C. F. and Mayor, R. (2005). Essential role of non-canonical Wnt signalling in neural crest migration. *Development* **132**, 2587-2597.
Deschamps, J. and van Nes, J. (2005). Developmental regulation of the Hox genes during axial morphogenesis in the mouse. *Development* **132**, 2931-2942.
Dull, T., Zufferey, R., Kelly, M., Mandel, R. J., Nguyen, M., Trono, D. and Naldini, L. (1998). A third-generation lentivirus vector with a conditional packaging system. *J. Virol.* **72**, 8463-8471.
Eastman, Q. and Grosschedl, R. (1999). Regulation of LEF-1/TCF transcription factors by Wnt and other signals. *Curr. Opin. Cell Biol.* **11**, 233-240.
Foerst-Potts, L. and Sadler, T. W. (1997). Disruption of Msx-1 and Msx-2 reveals roles for these genes in craniofacial, eye, and axial development. *Dev. Dyn.* **209**, 70-84.
Garcia-Castro, M. I., Marcelle, C. and Bronner-Fraser, M. (2002). Ectodermal Wnt function as a neural crest inducer. *Science* **13**, 13.
Gavin, B. J., McMahon, J. A. and McMahon, A. P. (1990). Expression of multiple novel Wnt-1/int-1-related genes during fetal and adult mouse development. *Genes Dev.* **4**, 2319-2332.
Hartmann, C. (2006). A Wnt canon orchestrating osteoblastogenesis. *Trends Cell Biol.* **16**, 151-158.
Hartmann, C. and Tabin, C. J. (2000). Dual roles of Wnt signaling during chondrogenesis in the chicken limb. *Development* **127**, 3141-3159.
Hatton, K. S., Mahon, K., Chin, L., Chiu, F. C., Lee, H. W., Peng, D., Morgenbesser, S. D., Horner, J. and DePinho, R. A. (1996). Expression and activity of L-Myc in normal mouse development. *Mol. Cell. Biol.* **16**, 1794-1804.
Helms, J. A. and Schneider, R. A. (2003). Cranial skeletal biology. *Nature* **423**, 326-331.
Hershkovitz, P. (1977). *Living New World Monkeys (Platyrrhini), Vol 1*. Chicago: University of Chicago Press.
Hirvonen, H., Makela, T. P., Sandberg, M., Kalimo, H., Vuorio, E. and Alitalo, K. (1990). Expression of the myc proto-oncogenes in developing human fetal brain. *Oncogene* **5**, 1787-1797.
Hoffman, J., Kuhnert, F., Davis, C. R. and Kuo, C. J. (2004). Wnts as essential growth factors for the adult small intestine and colon. *Cell Cycle* **3**, 554-557.
Hu, D., Marcucio, R. S. and Helms, J. A. (2003). A zone of frontonasal ectoderm regulates patterning and growth in the face. *Development* **130**, 1749-1758.
Hu, H., Hilton, M. J., Tu, X., Yu, K., Ornitz, D. M. and Long, F. (2005). Sequential roles of Hedgehog and Wnt signaling in osteoblast development. *Development* **132**, 49-60.
Hunt, P., Clarke, J. D., Buxton, P., Ferretti, P. and Thorogood, P. (1998). Stability and plasticity of neural crest patterning and branchial arch Hox code after extensive cephalic crest rotation. *Dev. Biol.* **198**, 82-104.
Hussein, S. M., Duff, E. K. and Sirard, C. (2003). Smad4 and beta-catenin co-activators functionally interact with lymphoid-enhancing factor to regulate graded expression of Msx2. *J. Biol. Chem.* **278**, 48805-48814.
Itah, R., Gitelman, I., Tal, J. and Davis, C. (2004). Viral inoculation of mouse embryos in utero. *J. Virol. Methods* **120**, 1-8.
Juriloff, D. M., Harris, M. J., McMahon, A. P., Carroll, T. J. and Lidral, A. C. (2006). Wnt9b is the mutated gene involved in multifactorial nonsyndromic cleft lip with or without cleft palate in A/WySn mice, as confirmed by a genetic complementation test. *Birth Defects Res. A Clin. Mol. Teratol.* **76**, 574-579.
Kengaku, M., Capdevila, J., Rodriguez-Esteban, C., De La Pena, J., Johnson, R. L., Belmonte, J. C. and Tabin, C. J. (1998). Distinct WNT pathways regulating AER formation and dorsoventral polarity in the chick limb bud. *Science* **280**, 1274-1277.
Kolpakova, E. and Olsen, B. R. (2005). Wnt/beta-Catenin-A canonical tale of cell-fate choice in the vertebrate skeleton. *Dev. Cell* **8**, 626-627.
Korinek, V., Barker, N., Moerer, P., van Donselaar, E., Huls, G., Peters, P. J. and Clevers, H. (1998a). Depletion of epithelial stem-cell compartments in the small intestine of mice lacking Tcf-4. *Nat. Genet.* **19**, 379-383.
Korinek, V., Barker, N., Willert, K., Molenaar, M., Roose, J., Wagenaar, G., Markman, M., Lamers, W., Destree, O. and Clevers, H. (1998b). Two members of the Tcf family implicated in Wnt/beta-catenin signaling during embryogenesis in the mouse. *Mol. Cell. Biol.* **18**, 1248-1256.
Kuhnert, F., Davis, C. R., Wang, H. T., Chu, P., Lee, M., Yuan, J., Nusse, R. and Kuo, C. J. (2004). Essential requirement for Wnt signaling in proliferation of adult small intestine and colon revealed by adenoviral expression of Dickkopf-1. *Proc. Natl. Acad. Sci. USA* **101**, 266-271.
Le Douarin, N. M., Creuzet, S., Couly, G. and Dupin, E. (2004). Neural crest cell plasticity and its limits. *Development* **131**, 4637-4650.
Levi, G., Mantero, S., Barbieri, O., Cantatore, D., Paleari, L., Beverdam, A., Genova, F., Robert, B. and Merlo, G. R. (2006). Msx1 and Dlx5 act independently in development of craniofacial skeleton, but converge on the regulation of Bmp signaling in palate formation. *Mech. Dev.* **123**, 3-16.
Liu, H., Mohamed, O., Dufort, D. and Wallace, V. A. (2003). Characterization of Wnt signaling components and activation of the Wnt canonical pathway in the murine retina. *Dev. Dyn.* **227**, 323-334.
Maretto, S., Cordenonsi, M., Dupont, S., Braghetta, P., Broccoli, V., Hassan, A. B., Volpin, D., Bressan, G. M. and Piccolo, S. (2003). Mapping Wnt/beta-catenin signaling during mouse development and in colorectal tumors. *Proc. Natl. Acad. Sci. USA* **100**, 3299-3304.
Martin, R. A., Jones, K. L. and Benirschke, K. (1996). Absence of the lateral philtral ridges: a clue to the structural basis of the philtrum. *Am. J. Med. Genet.* **65**, 117-123.
Monsoro-Burq, A. H., Wang, E. and Harland, R. (2005). Msx1 and Pax3 cooperate to mediate FGF8 and WNT signals during Xenopus neural crest induction. *Dev. Cell* **8**, 167-178.
Moriyama, A., Kii, I., Sunabori, T., Kurihara, S., Takayama, I., Shimazaki, M., Tanabe, H., Oginuma, M., Fukayama, M., Matsuzaki, Y. et al. (2007). GFP transgenic mice reveal active canonical Wnt signal in neonatal brain and in adult liver and spleen. *Genesis* **45**, 90-100.
Mugrauer, G., Alt, F. W. and Ekblom, P. (1988). N-myc proto-oncogene expression during organogenesis in the developing mouse as revealed by in situ hybridization. *J. Cell Biol.* **107**, 1325-1335.
Niemann, S., Zhao, C., Pascu, F., Stahl, U., Aulepp, U., Niswander, L., Weber, J. L. and Muller, U. (2004). Homozygous WNT3 mutation causes tetra-amelia in a large consanguineous family. *Am. J. Hum. Genet.* **74**, 558-563.
Noden, D. M. (1988). Interactions and fates of avian craniofacial mesenchyme. *Development* **103**, 121-140.
Nusse, R. (1999). WNT targets. Repression and activation. *Trends Genet.* **15**, 1-3.
Okubo, T., Pevny, L. H. and Hogan, B. L. (2006). Sox2 is required for development of taste bud sensory cells. *Genes Dev.* **20**, 2654-2659.
Oliver, T. G., Grasfeder, L. L., Carroll, A. L., Kaiser, C., Gillingham, C. L., Lin, S. M., Wickramasinghe, R., Scott, M. P. and Wechsler-Reya, R. J. (2003). Transcriptional profiling of the Sonic hedgehog response: a critical role for N-myc in proliferation of neuronal precursors. *Proc. Natl. Acad. Sci. USA* **100**, 7331-7336.
Oosterwegel, M., van de Wetering, M., Timmerman, J., Kruisbeek, A., Destree, O., Meijlink, F. and Clevers, H. (1993). Differential expression of the HMG box factors TCF-1 and LEF-1 during murine embryogenesis. *Development* **118**, 439-448.
Osumi-Yamashita, N., Ninomiya, Y., Doi, H. and Eto, K. (1994). The contribution of both forebrain and midbrain crest cells to the mesenchyme in the frontonasal mass of mouse embryos. *Dev. Biol.* **164**, 409-419.
Osumi-Yamashita, N., Ninomiya, Y. and Eto, K. (1997). Mammalian craniofacial embryology in vitro. *Int. J. Dev. Biol.* **41**, 187-94.
Reya, T., Duncan, A. W., Ailles, L., Domen, J., Scherer, D. C., Willert, K., Hintz, L., Nusse, R. and Weissman, I. L. (2003). A role for Wnt signalling in self-renewal of haematopoietic stem cells. *Nature* **423**, 409-414.
Ridanpaa, M., Fodde, R. and Kielman, M. (2001). Dynamic expression and nuclear accumulation of beta-catenin during the development of hair follicle-derived structures. *Mech. Dev.* **109**, 173-181.
Sasaki, T., Ito, Y., Xu, X., Han, J., Bringas, P., Jr, Maeda, T., Slavkin, H. C., Grosschedl, R. and Chai, Y. (2005). LEF1 is a critical epithelial survival factor during tooth morphogenesis. *Dev. Biol.* **278**, 130-143.
Satokata, I., Ma, L., Ohshima, H., Bei, M., Woo, I., Nishizawa, K., Maeda, T., Takano, Y., Uchiyama, M., Heaney, S. et al. (2000). Msx2 deficiency in mice causes pleiotropic defects in bone growth and ectodermal organ formation. *Nat. Genet.* **24**, 391-395.

Schneider, R. A. and Helms, J. A. (2003). The cellular and molecular origins of beak morphology. *Science* **299**, 565-568.
Slack, J. M., Holland, P. W. and Graham, C. F. (1993). The zootype and the phylotypic stage. *Nature* **361**, 490-492.
Trainor, P. A., Tan, S. S. and Tam, P. P. (1994). Cranial paraxial mesoderm: regionalisation of cell fate and impact on craniofacial development in mouse embryos. *Development* **120**, 2397-2408.
Trainor, P. A., Ariza-McNaughton, L. and Krumlauf, R. (2002). Role of the isthmus and FGFs in resolving the paradox of neural crest plasticity and prepatterning. *Science* **295**, 1288-1291.
Tucker, A. S., Matthews, K. L. and Sharpe, P. T. (1998). Transformation of tooth type induced by inhibition of BMP signaling. *Science* **282**, 1136-1138.
Vainio, S., Karavanova, I., Jowett, A. and Thesleff, I. (1993). Identification of BMP-4 as a signal mediating secondary induction between epithelial and mesenchymal tissues during early tooth development. *Cell* **75**, 45-58.
van Genderen, C., Okamura, R. M., Farinas, I., Quo, R. G., Parslow, T. G., Bruhn, L. and Grosschedl, R. (1994). Development of several organs that require inductive epithelial-mesenchymal interactions is impaired in LEF-1-deficient mice. *Genes Dev.* **8**, 2691-2703.
Veeman, M. T., Slusarski, D. C., Kaykas, A., Louie, S. H. and Moon, R. T. (2003). Zebrafish prickle, a modulator of noncanonical Wnt/Fz signaling, regulates gastrulation movements. *Curr. Biol.* **13**, 680-685.
Wang, J. and Shackleford, G. M. (1996). Murine Wnt10a and Wnt10b: cloning and expression in developing limbs, face and skin of embryos and in adults. *Oncogene* **13**, 1537-1544.
Willert, J., Epping, M., Pollack, J. R., Brown, P. O. and Nusse, R. (2002). A transcriptional response to Wnt protein in human embryonic carcinoma cells. *BMC Dev. Biol.* **2**, 8.
Wodarz, A. and Nusse, R. (1998). Mechanisms of Wnt signaling in development. *Annu. Rev. Cell Dev. Biol.* **14**, 59-88.
Young, N. M., Wat, S., Diewert, V. M., Browder, L. W. and Hallgrímsson, B. (2007). Comparative morphometrics of facial morphogenesis: implications for the aetiology of cleft lip. *Anat. Rec.* **290**, 123-139.
Yu, H. M., Jerchow, B., Sheu, T. J., Liu, B., Costantini, F., Puzas, J. E., Birchmeier, W. and Hsu, W. (2005). The role of Axin2 in calvarial morphogenesis and craniosynostosis. *Development* **132**, 1995-2005.
Zimmerman, K. A., Yancopoulos, G. D., Collum, R. G., Smith, R. K., Kohl, N. E., Denis, K. A., Nau, M. M., Witte, O. N., Toran-Allerand, D., Gee, C. E. et al. (1986). Differential expression of myc family genes during murine development. *Nature* **319**, 780-783.